Characterization of soil dust aerosol in China and its transport and distribution during 2001 ACE-Asia: 1. Network observations

X. Y. Zhang,[1] S. L. Gong,[1,2] Z. X. Shen,[1] F. M. Mei,[1] X. X. Xi,[3] L. C. Liu,[4] Z. J. Zhou,[5] D. Wang,[1] Y. Q. Wang,[1] and Y. Cheng[1]

Received 7 June 2002; revised 3 November 2002; accepted 6 January 2003; published 2 May 2003.

[1] Mass loading, 20 elemental concentrations, and time series of aerosol particles were investigated over the China Dust Storm Research (ChinaDSR) observational network stations from March to May 2001 during the intensive field campaign period of ACE-Asia. Four extensive and several minor dust storm (DS) events were observed. Mass balance calculations showed that 45–82% of the observed aerosol mass was attributable to Asian soil dust particles among the sites, in which Ca and Fe contents are enriched to 12% and 6%, respectively, in the Western High-Dust source regions compared with dust aerosols ejected from the Northern High-Dust source regions. For the latter areas, elemental contents exhibited high Si (30%) and low Fe (4%). For all major source areas and depositional regions, aluminium (Al) comprises 7% of Asian dust. Air mass back-trajectory analysis showed that five major transport pathways of Asian dust storms dominated dust transport in China during spring 2001, all of which passed over Beijing. Measurements also suggest that the sand land in northeastern China is a potential source for Asian dust. The size distribution for estimating vertical dust flux was derived from the observed surface dust size distributions in the desert regions. For particle diameters between 0.25 and 16 μm, a lognormal distribution was obtained from averaging observations at various deserts with a mass mean diameter of 4.5 μm and a standard deviation of 1.5. This range of soil dust constitutes about 69% of the total dust loading. The fractions for particles in the size ranges of <2.5 μm and >16 μm are around 1.7% and 30%, respectively. *INDEX TERMS:* 0305 Atmospheric Composition and Structure: Aerosols and particles (0345, 4801); 0322 Atmospheric Composition and Structure: Constituent sources and sinks; 0365 Atmospheric Composition and Structure: Troposphere—composition and chemistry; 3210 Mathematical Geophysics: Modeling; *KEYWORDS:* Asia, soil dust, observation, simulation, ACE-Asia

Citation: Zhang, X. Y., S. L. Gong, Z. X. Shen, F. M. Mei, X. X. Xi, L. C. Liu, Z. J. Zhou, D. Wang, Y. Q. Wang, and Y. Cheng, Characterization of soil dust aerosol in China and its transport and distribution during 2001 ACE-Asia: 1. Network observations, *J. Geophys. Res.*, *108*(D9), 4261, doi:10.1029/2002JD002632, 2003.

1. Introduction

[2] Desert regions in East Asia are widely considered to be the major sources for Asian dust according to present-day observations and rain-dust records in Chinese historical documents [*Merrill et al.*, 1994, 1989; *Prospero*, 1981; *Zhang*, 1984]. On the basis of 1994 observations, the most important sources for Asian soil dust have been identified as (1) the Western High-Dust Desert and (2) the Northern High-Dust Desert, with Taklimakan Desert and Badain Juran Desert in China as their centers, respectively [*Zhang et al.*, 1998]. Recently there has been increasing interest in connections among Asian dust, marine biogeochemical cycles, and climate [*Intergovernmental Panel on Climate Change* (*IPCC*), 2001]. Researchers [*Sokolik et al.*, 2001] have indicated that there is a gap between optical measurements and measurements of fundamental dust properties such as composition, particle size distribution, and transport patterns. Remote sensing (e.g., Total Ozone Mapping Spectrometer (TOMS) and advance very high resolution radiometer (AVHRR)) requires detailed chemical and physical properties of dust aerosols in order to correctly retrieve the aerosol optical depth in addition to their spatial and temporal distributions. These properties are complicated further by the fact that the dust aerosol may interact with or form stratified layers with anthropogenic aerosols such as sul-

[1]State Key Laboratory of Loess and Quaternary Geology, Institute of Earth Environment, Chinese Academy of Sciences, XiAn, China.
[2]Air Quality Research Branch, Meteorological Service of Canada, Toronto, Ontario, Canada.
[3]College of Resource and Environment, Lanzhou University, Lanzhou, China.
[4]Institute of Cold and Arid Environment and Engineering Research, Chinese Academy of Sciences, Lanzhou, China.
[5]Climate Data Centre, National Meteorological Canter, China Metrology Administration, Beijing, China.

0148-0227/03/2002JD002632$09.00

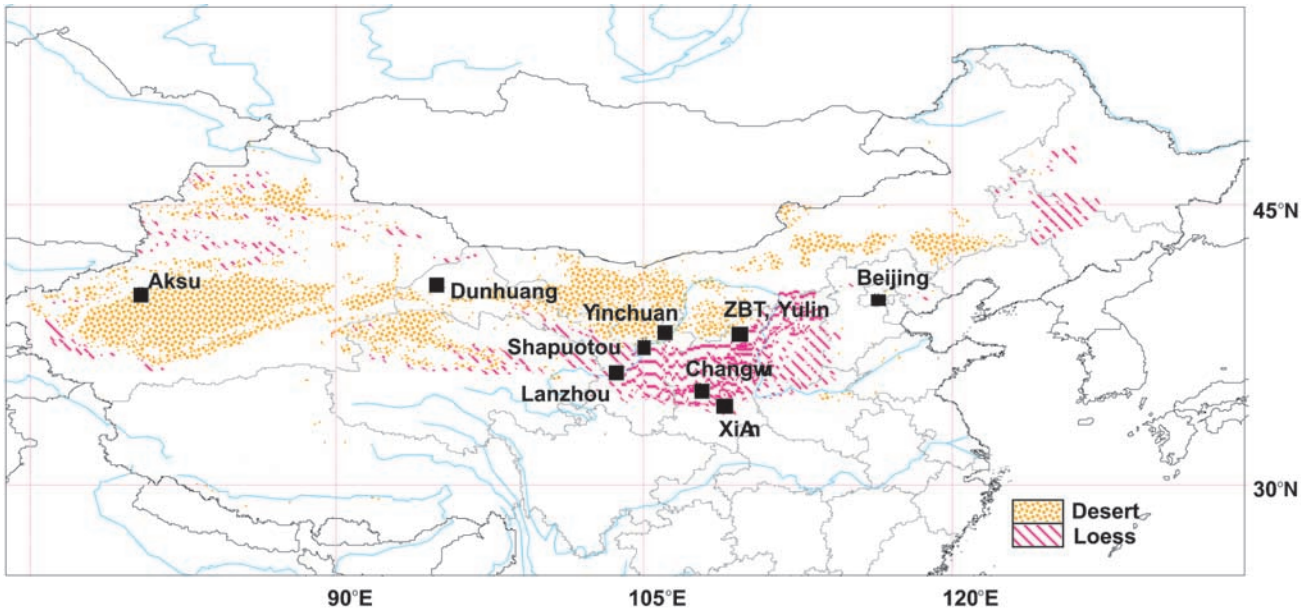

Figure 1. Network sites of the ground-based aerosol sampling for the China Dust Storm Research (ChinaDSR).

phate and organics. A detailed characterization of Asian aerosols requires the combination of observational data and mathematical models in order to take these complicated processes into consideration and to establish the spatial and temporal distribution of physical and chemical properties. With such an approach it may be possible to correctly address the impact of soil dust on climate and air quality problems.

[3] Understanding the chemical and physical properties of dust aerosol in the source regions is the key component to narrowing this gap. The lack of data from source regions with which to verify soil dust simulations has hindered the progress of modeling activities on soil dust impacts. Measurements of dust aerosols with respect to their time series, spatial distribution, and physical/chemical characterization are required for more accurate estimates of source strength, optical calculations, and model validations. Observations enhance not only our understanding of particle character, but also the temporal (synoptic to interannual) variability of windblown mineral dust over the most important Asian dust depositional areas [*Andreae*, 1995; *Overpeck et al.*, 1996; *Tegen et al.*, 1996].

[4] As part of an international campaign to understand Asian aerosols and their impact on climate, the Asia Pacific Regional Aerosol Characterization Experiment (ACE-Asia) was carried out off the coasts of China, Japan, and Korea and within China during spring 2001. Coordinated with the intensive field campaign period of ACE-Asia, China Dust Storm Research (ChinaDSR) observational network stations were operated to measure the aerosols across China at desert source regions and downwind reception sites.

[5] Here we present the daily aerosol observations from six sites in hyperarid, semiarid, urban, rural, and coastal areas of China, and particulate matter <10 μm in diameter (PM-10) burden at four Chinese cities during spring 2001. The specific objectives of the studies reported here were to (1) evaluate the chemical composition of bulk aerosol samples and estimate the Asian dust fractions; (2) investigate temporal variations in aerosol particles, Asian dust aerosol, and dust-derived elements, during dust storm events; (3) evaluate the composition of Asian dust collected at the two most important sources; (4) identify the transport pathways of dust; and (5) determine surface dust size distribution in the desert regions for source strength estimation. These observations will be used to initialize and validate a simulation model in a companion paper [*Gong et al.*, 2003] in which the transport and distribution of Asian soil dust within China and downwind as far afield as the mid-Pacific and North America are examined.

2. Sampling Network and Analysis Methods

[6] Since February 2001, a network of ground-based aerosol sampling stations for the China Dust Storm Research (ChinaDSR) has been established (Figure 1) in hyperarid, semiarid, urban, rural, and coastal areas of China. Some sites, like Zhenbeitai (ZBT), Yulin and Dunhang (DH), Qingdao, and Beijing, are also among the sites of the ACE-Asia Ground Station Network. Observations of physical and chemical characteristics and time series of soil dust aerosol were made at selected sites (denoted by solid squares in Figure 1). The detailed descriptions of each site and the sampling methods are summarized in Table 1.

[7] Two sampling methods are used in the network observations: a continuous RP-2025 air sampler and a bulk aerosol sampler. The RP-2025 air sampler (R&P Co., Inc., Albany, New York) has an automatic filter-changing system with a capacity of up to 16 filters (Teflo membrane filter, Cole-Parmer Instrument Company, Vernon Hills, Illinois) associated with an active volumetric flow-control system. The sampler can also record 16 days of interval data (the 5-min averages of the filter temperature, ambient temperature, ambient pressure, ambient relative humidity (RH), wind speed, wind direction, and average flow rate)

Table 1. Network Descriptions for the China Dust Storm Research (ChinaDSR) in Spring of 2001 During ACE-Asia IOP

Sampling Station	Site Description	Sampling Period	Instrument and Flow Rate	Sampling Time and Height
Aksu in Xinjiang (40°16′N, 80°28′E); annual precipitation, <50 mm; mean temperature, ~10°C	1028 m above sea level; 80 km east of Aksu city (Xinjiang province, China); located in a hyperarid area at northern margin of Taklimakan desert	13 May to 3 June	Andersen AN200, ~26.3 L min^{-1}	18 daytime (normally from 0900 to 1700 LT) bulk aerosol samples collected from a 20-m-tall building
Dunhuang (DH) (40°30′N, 94°49′E); annual precipitation, ~50 mm; mean temperature, ~10°C	1380 m above sea level; 25 km southeast of Dunhuang city (Gansu province, China); located in a hyperarid area at Kumtag Desert	29 April to 31 May	Andersen AN200, ~26.3 L min^{-1}	30 daytime (normally from 1000 to 1600 LT) bulk aerosol samples collected from a 10-m-tall building
Zhenbeitai (ZBT), Yulin (38°17′23″N, 109°42′18″E); annual precipitation, 300–400 mm; mean temperature, ~8°C	1135 m above sea level; 10 km north of Yulin (Shaanxi Province, China); located along the southeastern edge of Mu Us desert. The areas to the north of ZBT are in a vast hyperarid region of northern China.	19 Feb. to 21 May	RP-2025, ~16.7 L min^{-1}	58 12-hour (daytime) samples collected under northerly wind flow from a 20-m-tall tower at ZBT
Changwu (CW) (35°12′N, 107°40′30″E); annual precipitation, ~590 mm; mean temperature, ~9°C	1220 m above sea level; 100 km away from XiAn city, located on the midwest of the Loess Plateau	8 March to 31 May	RP-2025, ~16.7 L min^{-1}	85 daytime (0600–0800 LT and 1100–1300 LT) bulk aerosol samples collected from a 20-m-tall building
Lanzhou (36°03′N, 103°53′E); annual precipitation, 315 mm; mean temperature, 9.3°C	1518 m above sea level; site in urban area of Lanzhou city, located on the northwest of the Loess Plateau	14–15, 19–20 April; 21–24 May	KB-120, ~120 L min^{-1}	28 daily TSP loadings, each averaged from ~10 bulk samples (sampling time normally ranged from 0000 to 2400 LT) collected from a 10-m-tall building during DS days
Shapuotou (37°30′N, 105°E); annual precipitation, <50 mm; mean temperature, ~10°C	1335 m above sea level; 22 km west of Zhongwei county city (Gansu province, China); located in southern margin of Tengger desert	18–25 March; 4, 13, 28 April; 5–14 May	Sibata, HV1000F ~1000 L min^{-1}	14 daytime bulk aerosol samples collected from a 20-m-tall building

and can work well under the condition of −40°C. Stations at Zhenbeitai and Changwu were equipped with the RP-2025 (Table 1).

[8] The bulk aerosol samples were taken by filter holder with a pump of Andersen cascade impactor (Andersen AN200) on a Teflo membrane filter for Aksu and Dunhuang, by a single stage aerosol sampler KB-120 (Laoshan Institute for Electronic Equipment, Qingdao, China) on a Whatman 41 filter (Whatman International Limited, Maidstone, England) for Lanzhou, and by a high-volume air sampler (Sibata HV1000F) with PTFE-filter (Advance, PTFE50) for Shapuotou. Table 1 lists the flow rates and other sampling conditions for each of the instruments. Cross calibration of all the bulk instruments has been done, and consistency among the bulk samplers was checked regularly. All bulk sample filters were gravimetrically weighted to obtain the aerosol mass concentrations. Each filter was stored in a petri dish and placed into a silica gel desiccator for 24 hours to equilibrate to the temperature and relative humidity held at constant values between 20°C and 23°C (±2°C) and 20–30% (±2%), respectively. Gravimetric weighting was then made on a Mettler Balance Model 3 (Mettler Toledo Instruments Co., Ltd., Switzerland) with 1 μg resolution. Within the balance room a small silica gel container was placed, and the temperature and RH were held as the same condition to that of the silica gel desiccator. This weighing procedure was repeated three times for the same filter separated by a 24 equilibration. A mean net mass for each filter was obtained by averaging the three duplicated data. The difference among the three repeated weightings was allowed less than 10 μg for a valid blank filter and less than 30 μg for an aerosol filter sample.

[9] The bulk samples from Aksu, DH, ZBT, and CW were also analyzed directly using a proton induced X-ray emission (PIXE) method to obtain the elemental concentrations. The PIXE analyses were performed using the 2.5 MeV protons with a 50 nA beam current produced by 2 × 1.7 MV tandem accelerator at Beijing Normal University (for details, see *Zhang et al.* [1993]). Through these procedures, concentrations of 20 elements were established: Al, As, Br, Ca, Cl, Cr, Cu, Fe, K, Mg, Mn, Ni, P, Pb, S, Se, Si, Ti, V, and Zn. The data were corrected for backgrounds from blank filters.

[10] The PM-10 loads at Yinchuan (106°11′N, 38°18′E), Lanzhou (36°03′N, 103°53′E), XiAn (34°11′N, 108°34′E), and Beijing (39°34′N, 116°10′E) for 1 March to 31 May, 2001, were deduced from the ground air quality index (AQI) reports in major Chinese cities (State Environmental Protection Administration, available at http://www.zhb.gov.cn/index4.htm). On the basis of the technological rules related with to the Ambient Air Quality Daily Report by the China Environmental Protection Monitoring Center, the following formula was used to derive the PM-10 data from API of PM10.

$$C = \left[(I - I_{\text{low}})/(I_{\text{high}} - I_{\text{low}})\right] \times (C_{\text{high}} - C_{\text{low}}) + C_{\text{low}}, \quad (1)$$

where C is the concentration of PM-10. The I_{low} and I_{high} represent API grading limited value lower and larger than I (API index), respectively; C_{high} and C_{low} denote the PM-10 concentrations corresponding to I_{high} and I_{low}, respectively. Although the equivalent PM-10 concentrations (EPMs) are contributed from all particulate sources, this EPM is a good

Table 2. Observed Concentrations of TSP, 20 Elements, Estimated Asian Dust (AD) Loading and Percentages of Eight Major Dust Elements in AD Particles at Four Sites During Spring of 2001

		Aksu, May 2001 (n = 18)			Dunhuang, April to May 2001 (n = 30)			Zhenbeitai, Spring 2001, northerly wind (n = 58)			Changwu, Spring 2001 (n = 85)		
	Unit[a]	Mean (SD)	EF_{crust}[b]	% of AD[c] (SD)	Mean (SD)	EF_{crust}	% of AD (SD)	Mean (SD)	EF_{crust}	% of AD (SD)	Mean (SD)	EF_{crust}	% of AD (SD)
TSP	μg	926 (825)			317 (513)			257 (320)			210 (136)		
Al	μg	24 (24)	1.0	5.9 (0.3)	17 (26)	1.0	6.9 (0.8)	14 (17)	1.0	7.4 (1.4)	10 (8.1)	1	6.6 (0.5)
As	ng	116 (89)	386		99 (101)	1025		115 (110)	621		110 (71)	1116	
Br	ng	36 (52)	ND[d]		30 (34)	ND		40 (54)	ND		28 (27)	ND	
Ca	μg	49 (48)	5.5	12 (0.6)	16 (22)	3.1	7.7 (1.7)	11 (12)	2.3	6.2 (1.4)	11 (8.2)	3.1	7.6 (1.0)
Cl	μg	4.9 (3.7)	ND		0.83 (3.7)	ND		0.39 (0.52)	ND		0.47 (0.49)	ND	
Cr	ng	56 (84)	3.8		22 (56)	1.5		11 (37)	2.5		6.9 (13)	1.8	
Cu	ng	112 (150)	12		100 (124)	14		44 (77)	11		33 (40)	12	
Fe	μg	25 (27)	2.3	5.9 (0.3)	60 (106)	1.4	4.0 (0.9)	7.3 (8.2)	1.2	3.9 (0.5)	6.2 (4.8)	1.4	4.0 (0.4)
K	μg	13 (13)	1.5	3.0 (0.1)	4.5 (6.7)	0.91	2.1 (0.4)	3.5 (3.8)	0.77	1.9 (0.3)	3.8 (2.4)	1.3	2.8 (1.0)
Mg	μg	12 (13)	2.9	2.8 (0.1)	3.7 (6.4)	1.5	1.7 (1.5)	3.6 (8.4)	1.9	1.5 (1.3)	2.1 (2.2)	0.9	1.0 (1.0)
Mn	μg	0.44 (0.45)	2.3	0.1 (0.02)	0.17 (0.25)	2.1	0.1 (0.05)	0.17 (0.17)	2.2	0.1 (0.05)	0.14 (0.09)	2.2	0.1 (0.05)
Ni	ng	192 (245)	30		73 (116)	22		67 (74)	25		49 (52)	22	
P	μg	1.5 (1.1)	9.8		0.84 (0.68)	15		1.0 (0.95)	11		0.92 (0.53)	13	
Pb	ng	159 (312)	23		70 (123)	50		64 (86)	40		80 (114)	53	
S	μg	3.3 (1.7)	ND		1.4 (1.5)	ND		1.4 (1.0)	ND		3.1 (2.6)	ND	
Se	ng	83 (143)	5.7		30 (33)	11		58 (73)	14		39 (43)	11	
Si	μg	97 (95)	1.1	24 (0.5)	65 (96)	1.1	29 (2.7)	58 (62)	1.1	32 (1.9)	44 (34)	1.1	29 (2.0)
Ti	μg	2.1 (2.2)	2.3	0.5 (0.03)	1.3 (2.2)	1.8	0.5 (0.13)	1.1 (1.5)	2.1	0.6 (0.2)	0.76 (0.63)	1.9	0.5 (0.09)
V	ng	44 (138)	1.4		16 (47)	0.84		10 (36)	0.92		5.0 (7.8)	0.8	
Zn	ng	42 (61)	2.0		20 (37)	3.1		28 (47)	4.2		55 (74)	12	
Estimated AD	μg	412 (410)			224 (334)			186 (204)			152 (116)		
Sum of trace elements	μg	2.4 (2.1)			1.3 (1.1)			1.8 (1.4)			1.3 (0.65)		
AD of TSP	%	45			67			82			69		

[a]Per standard cubic meter.
[b]Al as reference element.
[c]Asian dust, estimated by material balance cal.
[d]No data.

indication of relative dust concentrations across China, especially for dust episodes.

3. Results and Discussions

3.1. Elemental Composition and Mass Balance of Observed Aerosol Particles

[11] Observed concentrations of TSP, 20 elements, estimated loading and percentages of eight major dust elements, Al, Ca, Fe, K, Mg, Mn, Si, and Ti are presented in Table 2 for three desert sites (Aksu, Dunhuang, and ZBT; Figure 1) and one loess site (Changwu; Figure 1) for spring 2001. In general, the higher elemental concentrations were always found for the eight typical dust elements (Table 2). The elemental proportions of eight elements closely resemble those of material from the Earth's upper continental crust [*Taylor and McLennan*, 1995]. This is demonstrated by the calculation of enrichment factors relative to crustal rock using Al as a reference element (EF_{crust} = $(element/Al)_{air}$/$(element/Al)_{crust}$). The EF_{crust} values, all close to unity with maximum values less than 5, indicate that the eight elements in our samples were dominated by mineral dust (Table 2). High correlations (r ranged from 0.91 to 0.99 in Figure 2) between all the dust elements with Al verify the crustal origin of these eight dust elements.

[12] Compared with the dust-derived elements, the EF_{crust} values for As, Cu, Ni, P, Pb, and Se are much larger than 5, suggesting the influence of noncrustal sources. EF_{crust} values for Cr, V, and Zn are also smaller than 5, except for Zn at Changwu. This reflects the lesser significance of these typical anthropogenic elements in China [*Zhang et al.*, 1993, 1998] and the relatively clean air in desert and loess regions.

[13] Not surprisingly, the higher concentrations were always associated with all the eight dust-derived elements, in which Si, Ca, Al, Fe, K, and Mg have higher loads (Table 2). The loadings of Ca, Fe, K, Mg, and Si were similar at DH, ZBT, and CW but were remarkably different at Aksu. For instance, the Ca concentrations were 16, 11, and 12 μg m^{-3} at DH, ZBT, and CW, respectively, and 49 μg m^{-3} at Aksu. This suggests that the elemental signature of dust particles derived from western desert sources of Asian dust is different from other sources [*Zhang et al.*, 1997, 1996]. Similarities in elemental composition of dust aerosol from ZBT and CW (Table 2) suggest that dust transport was more northerly during relatively mild climate conditions such as interglacials or the present day [*Zhang et al.*, 1999].

[14] The sum of the other elements or trace elements (Tr Ele) in Table 2 does not show high concentrations in the source region (1.3–2.4 μg m^{-3}). The Pb burden at the four sites (64–159 ng m^{-3} (Table 2)) is at least tenfold less than at Chinese urban sites during springtime [*Zhang et al.*, 2002], again indicative of the clean air conditions in Asian dust source regions.

[15] Normally there are five categories of suspended particulates contributing to TSP over continental sites: (1) geological materials, mainly Asian dust (AD) [*Zhang et al.*, 2002], and associated species (consisting of oxides of Al,

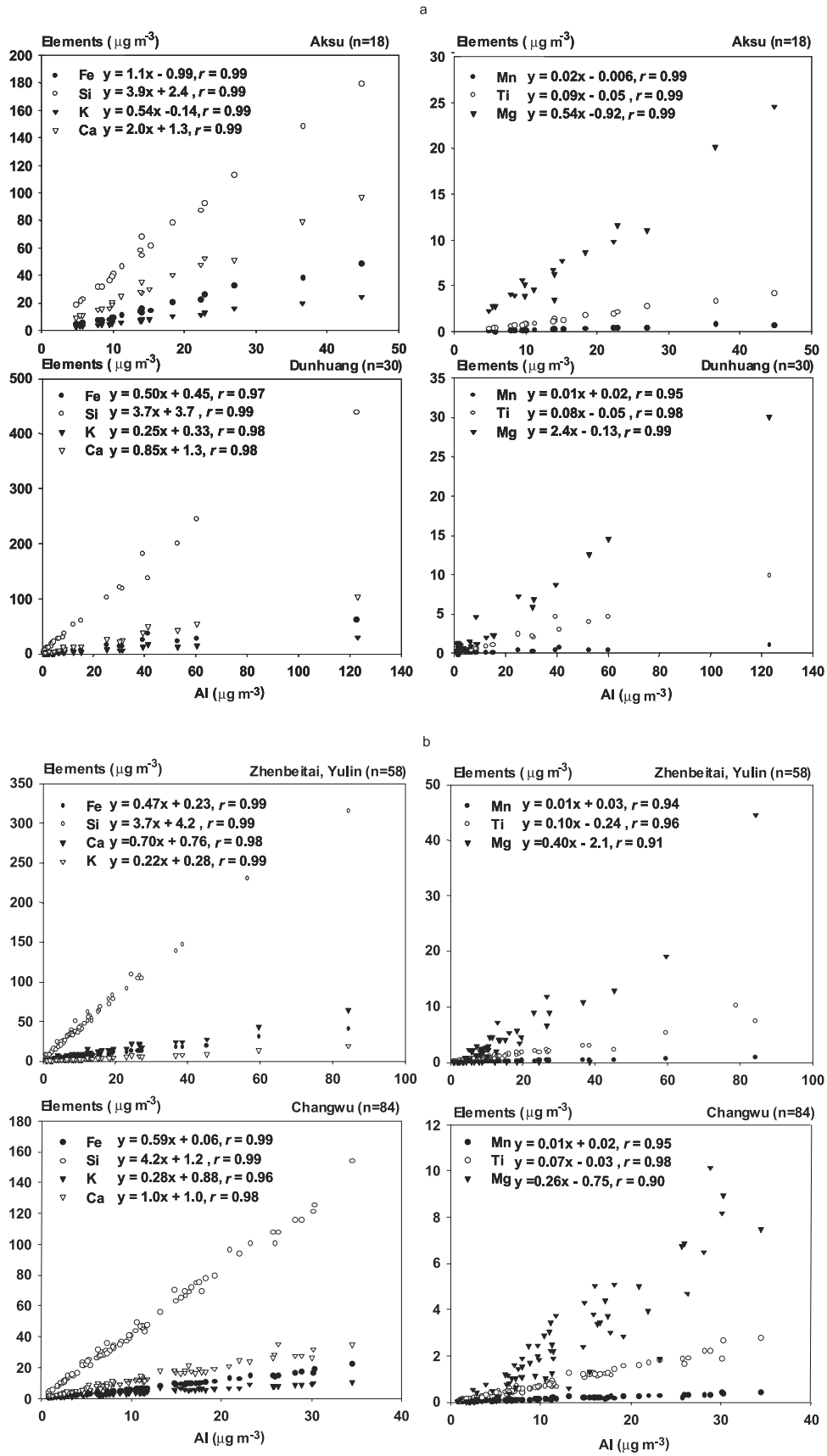

Figure 2. Correlations between dust elements with aluminum in ground-based aerosol particle at Chinese desert and the loess regions: (a) Aksu and Duhuang (DH) data. (b) Zhenbeitai (ZBT) and Changwu (CW) data.

Si, K, Ca, Ti, and Fe, and trace elements), (2) particulate sulphates, (3) aerosol nitrates, (4) ammonium products, and (5) carbonaceous material [*Solomon et al.*, 1989]. Elemental analyses are particularly valuable for assessing the contributions from the geological material, most of which here are assumed to be Asian dust aerosol . As no data on sulphate, nitrate, ammonium and carbonaceous aerosols were available at this moment, the mass balances of the aerosol particles at these four sites were based solely on the analysis of the TSP mass concentrations and the burden of dust elements and various trace elements. Therefore, in order to estimate the Asian dust aerosol, the sum of the aluminum, silicon, calcium, and iron oxides was calculated using $1.89 \times \mathrm{Al} + 2.14\ \mathrm{Si} + 1.4 \times \mathrm{Ca} + 1.43 \times \mathrm{Fe}$ [*Solomon et al.*, 1989]. The estimated seasonally averaged loading of Asian dust aerosol and its percentage of the TSP, sum of the trace elements are also presented in Table 2. As the composition of the Asian mineral dust is reasonably well known [*Geological Soil Standard*, 1984; *Zhang et al.*, 1993, 1997, 1998], titanium, magnesium, manganese, and potassium oxides were added to estimate the amount of geological Asian dust particles.

[16] Asian dust aerosols constitute about 45, 67, 82, and 69% of the average TSP at Aksu, DH, ZBT, and CW, respectively (Table 2), suggesting ~10–50% of aerosol fractions cannot be attributable to soil dust particles, even in the source regions of Asian dust. At urban XiAn this dust percentage normally ranges from 37 to 45% throughout all seasons, with 45% in springtime. The nondust fractions were mainly attributable to sulphate, nitrate, elemental, organic carbon aerosol particles and ammonium products from coal combustion, motor vehicle, biomass burning, and agriculture activities [*Zhang et al.*, 2002]. At Dunhuang the contributions of Asian dust to the total aerosol mass were estimated to be ~80% and 62% during dust and nondust conditions, respectively; these percentage were ~87% and 74% at Zhenbeitai, and ~75% and 64% at Changwu for dust and nondust periods, respectively. A separate paper is being prepared with an annual data set from these stations to investigate the seasonal variations of the dust contributions from dust and nondust periods.

[17] Northerly wind samples collected at ZBT may explain the relatively high fraction of Asian dust at this site. Taking the estimated geological material as representative Asian dust aerosol; Aksu to represent the western desert sources; DH and ZBT to represent sources in the northern desert [*Zhang et al.*, 1997, 1996]; and CW to represent the depositional loess region, the aluminum fraction can then calculated. Values among regions are remarkably similar, with 5.9, 6.9, 7.4, and 6.6% for Aksu, DH, ZBT, and CW, respectively, with mean value ~7% of the total dust mass (Table 2). Mn and Ti also show similar percentages among regions with means of ~0.1 and 0.5, respectively. Percentage mass of Ca, Fe, K, Mg, and Si are 12, 6, 3, 3, and 24%, respectively, for western desert sources represented by Aksu data and 7, 4, 2, 2, and 30%, respectively, for northern desert sources represented by DH and ZBT data (Table 3). Clearly, western desert sources are characterized by high Ca while northern sources are high in Si. This suggests that major source regions of Asian dust have different source profiles and signatures. In comparison, the mean percentages with standard deviations for the depositional loess area are 7, 8, 4, 3, 1, 0.1, 29, and 0.5% for Al, Ca, Fe, K, Mg, Mn, Si, and Ti, respectively (Table 3).

Table 3. Source Profiles, Weight Percent, of Dust Elements in Asian Dust Aerosol Mass

Asian Dust Sources	Al	Ca	Fe	K	Mg	Mn	Si	Ti
Western High-Dust Source[a]	7	12	6	3	3	0.1	24	0.5
Northern High-Dust Source[b]	7	7	4	2	2	0.1	30	0.5
Loess area	7	8	4	3	1	0.1	29	0.5

[a]Desert regions in western China and surrounding areas with Taklimakan Desert as its center.

[b]Desert regions with relative high dust depositional flux to other northern desert in northern China with Badain Juran Desert as its center [*Zhang et al.*, 1997; *Zhang et al.*, 1996].

3.2. Dust Storm Events Observed in China During Spring of 2001

[18] Four major and two minor DS events were observed during spring 2001. Another two DS events observed at Aksu and DH were confined to the source areas (termed as source DS (SDS)). These events were apparent in time series of total suspended particle (TSP) loading, elemental composition, PM-10 from the State Environmental Protection Administration (SEPA) of China. For example, the time series of TSP at CW (Figure 3f), a depositional area on the Loess Plateau (Figure 1), exhibited three high aerosol episodes between 13 and 27 March (DS2); 5 and 20 April (DS3); and 29 April 29 and 5 May (DS4). During these periods, TSP values were continually higher than the observed spring daily average (210 $\mu g\ m^{-3}$, Figure 3f). Higher concentrations exceeding the average were also found for the eight typical dust elements (Al, Ca, Fe, K, Mg, Mn, Si, and Ti). For instance, the Si loading continually exceeded the average level (44 $\mu g\ m^{-3}$) during the same high aerosol episodes (Figure 3f), confirming that the episodes were indeed associated with increased Asian dust particle loading. The other typical dust elements (Al, Ca, Fe, K, Mn, Mg, and Ti), due to the high correlations with each other (Figure 2), also show similar temporal variations to Si (Figure 3). On 23 May 2001, both the TSP and Si burdens exceeded mean levels, suggesting a high dust day occurred (DS6 in Figure 3). Because of the southerly paths of the surface air mass observed (by air mass back-trajectory analyses described in the next section) on some days (e.g., 19 March, 1, 2, 3, 4, 17, and 29 April, and 6 and 23 May), the higher TSP and elemental loading was not attributable to the DS contributions.

[19] The first DS event (DS1 in Figure 3) of spring 2001 occurred from 1 to 6 March. TSP and Si loading was higher than the average observed under northerly wind flows at ZBT, Yulin, a desert source site (Figure 1). Loading of PM-10 at Yinchuan, TSP at Shapuotou (SPT) (Figure 3d), both TSP and PM-10 at Lanzhou (Figure 3e), and PM-10 at XiAn (Figure 3g) and Beijing (Figure 3h) also exceeded the average. This indicates that DS1 was a relatively intense and extensive DS event that had an impact over large areas of China.

[20] DS2 from 13 to 27 March was another group of dust storm events observed at almost all the network sites (Figures 3c–3h). At ZBT, unlike other sites, high TSP and Si concentrations were only observed from 22 to 26

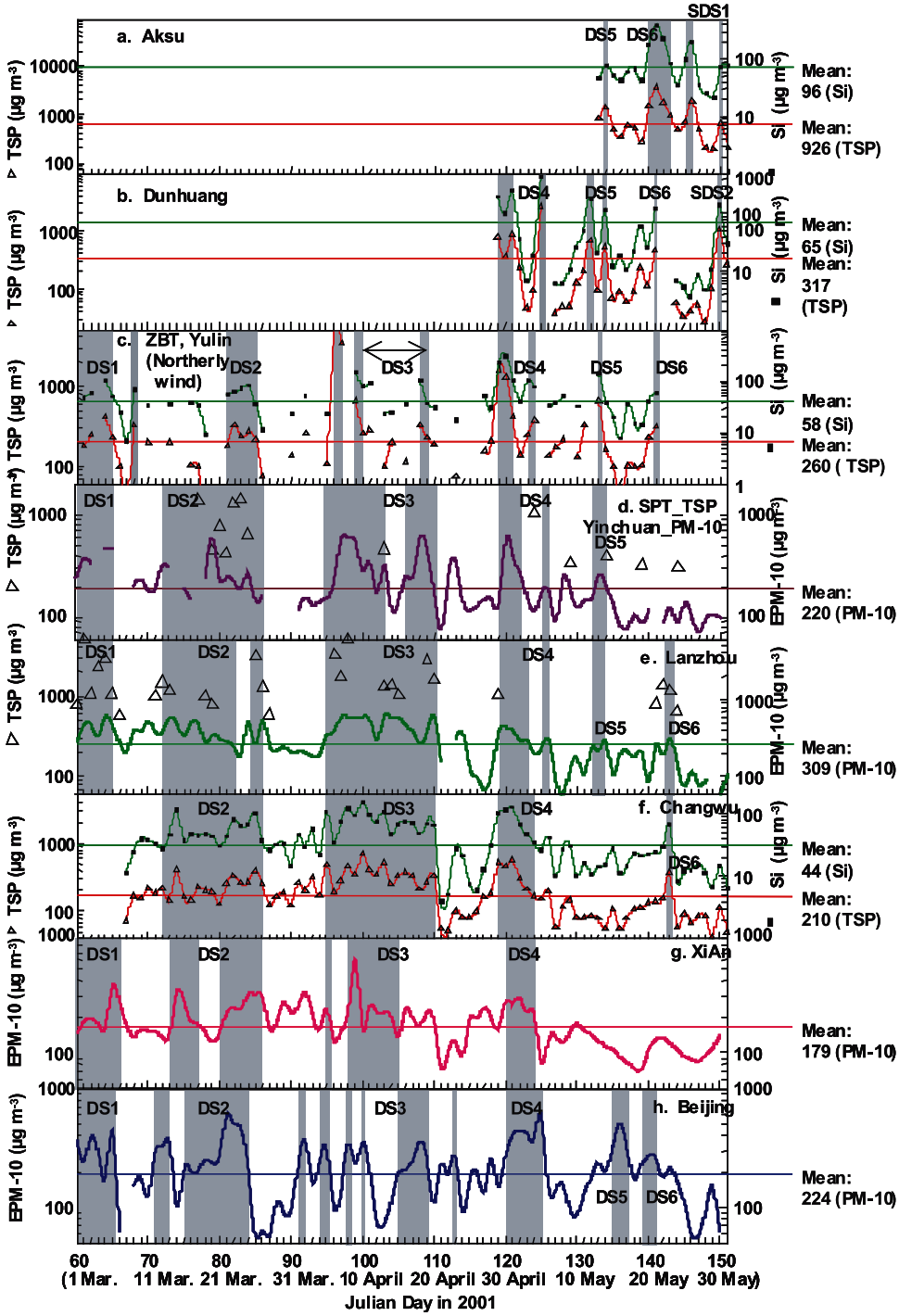

Figure 3. Time series of concentrations of TSP, dust elemental Si, and PM-10 (EMP-10) observed at Chinese desert regions (Aksu, Figure 3a; Dunhuang, Figure 3b; ZBT, Figure 3c; SPT and Yinchuan, Figure 3d), urban city near the desert source and at the northwest margin of the Loess Plateau (Lanzhou, Figure 3e), the loess site (Changwu, Figure 3f), urban city at southern margin of the Loess Plateau (XiAn, Figure 3g), and urban city in historical northeastern area (Beijing, Figure 3h) between 1 March and 31 May of 2001. The open circles in Figures 3b and 3c denote the sum of the eight size-segregated Si loadings.

March (Figure 3c). This is probably because only northerly wind samples were collected; some dust samples, originated from major sources, but reaching ZBT from the south in their final phase of transport, were not collected by the sampler. Lower concentrations were only observed on one day at Lanzhou (Figure 3e) and on two days at XiAn (Figure 3g) during the DS2 period. There was one dusty day, 12 March, occurring in advance of DS2 at Beijing. This

event was probably due to the transport of dust particles on that day via Mongolia and across the northern slopes of Yin Mountain, directly to Beijing (Figure 5d).

[21] The most intense and persistent DS event (DS3) occurred from 5 to 20 April and was observed at all sites (Figures 3c–3h). Again due to northerly wind samples collected at ZBT, there were 6 days with low dust loads during the episode. At most sites the episode was ~16 days in duration. Because trajectories were from the south, the elevated loads of EPM-10, TSP, and dust elements (not marked with shading in Figure 3) at XiAn, Beijing, CW, Lanzhou, and Yinchuan before DS3 and on subsequent days during the spring are not considered to be attributable to contributions from DS events.

[22] DS4 occurred between 29 April and 5 May. Both at DH and ZBT, higher TSP and Si loadings were observed on 29 April (Figures 3b and 3c). On the same day, higher loadings of aerosols and dust aerosols were observed at Yinchuan and Lanzhou; one day later the same peak was observed at Changwu, XiAn, and Beijing (Figures 3d–3h). During DS4, there were fewer dust days found at source or near source sites such as DH, ZBT, Yinchuan, and Lanzhou. However, at CW, XiAn, and Beijing, the three typical depositional areas, the high aerosol loads lasted through the entire DS4 event. At Beijing one more dust day was observed than CW and XiAn during DS4. The air mass moved eastward on 5 May (Figure 5d) to Beijing and did not reach CW and XiAn.

[23] In addition to the DS1 to DS4 events, there was another relatively short DS episode in China, DS5, lasting two to three days, from 11 to 14 May. This event was observed at Aksu, DH, ZBT, Yinchuan, and Lanzhou (Figures 3a–3e). This DS event was confined mostly to source areas with the source strength at DH and ZBT compatible to DS4, but the spatial extent and duration of the event were less than observed for DS4. At Beijing, the dust days occurred from 15 to 17 May. Back-trajectory analysis indicates that the contributions to these three dust days were associated with an air mass reaching Beijing via the Yin Mountain northern slope from the Mongolian Desert (Figure 5d).

[24] On 19 May, another small DS event (DS6) occurred at DH and subsided the next day (Figure 3b). It developed again at Aksu, DH, Yulin, on 21 May (Figures 3a–3c) and lasted until 23 May at Aksu. Relatively high aerosol concentrations were then observed at Lanzhou and CW on 22 May and lasted to 23 May (Figures 3f and 3e). At Beijing, the dust episode lasted from 19 to 21 May (Figure 3h). At the end of May, one high aerosol day that exceeded mean levels of both TSP and Si, was identified at Aksu only on 26 May (source DS1, i.e., SDS1 in Figure 3a). Another SDS (SDS2) was also observed at both Aksu and DH on 30 May.

[25] Beijing experienced relatively higher average PM-10 levels than XiAn, Yinchuan, and CW during the entire spring of 2001. There were at least 43 dust-event days in Beijing compared with 32 in XiAn. Before the extensive DS2, DS3, and DS4 episodes, at least one DS event and one dusty day occurred at Beijing, which was not found at other cities in the depositional regions. During DS5 and DS6, the high dust days were also observed at Beijing (Figure 3h). One of the possible reasons for the higher intensity and more frequent dust events at Beijing was that more transport paths were available for dust to reach Beijing. This is further discussed in section 3.3.

[26] During nondust storm (N-DS) days with calm or weak wind conditions, the monthly mean background aerosol concentrations were from 130 to 150 $\mu g\ m^{-3}$ in March and April, respectively, and 80 $\mu g\ m^{-3}$ in May, at CW. Thereafter, background TSP loading were about 60, 40, and 50 $\mu g\ m^{-3}$ during June, July, and August of 2001, respectively.

[27] At one desert source site (ZBT), TSP loadings under northerly wind flows showed at least 29 dust days with Si levels higher than the springtime average 260 μg TSP m^{-3}, and 58 μg Si m^{-3} (Figure 3c). As at CW, high loads were also observed for the other seven dust elements. In comparison with DS, nondust days with calm or weak northwesterly or northeasterly winds had background aerosol loadings of 93 $\mu g\ m^{-3}$ in March, 150 $\mu g\ m^{-3}$ in April, and 91 $\mu g\ m^{-3}$ in May.

[28] At DH, the 1-month data set exhibited 12 dust days with TSP and Si loads both exceeding the mean value of 317 μg TSP m^{-3}, and 65 μg Si m^{-3} in May. These TSP and Si levels are much lower than that at Aksu with loads of 926 $\mu g\ m^{-3}$ and 96 $\mu g\ m^{-3}$ for TSP and Si, respectively.

[29] The mass ratio of Si to Al is an indictor of the origin of an air mass arriving at a monitoring station. Although the Si:Al ratio has an averaged value of around 4.0 (Table 2) for all stations during the entire spring of 2001, the ratio changes substantially depending on the trajectories of each mass. Figure 4 shows that time series of the Si:Al during spring 2001 for four stations. The high Si:Al is usually associated with an air mass originated from northern deserts, while the low rations with an air mass originated from the western desert source regions. More discussion about the air mass trajectory is given in the next section.

3.3. Transport Pathways of Dust Storms in China

[30] Air mass back-trajectories, generated with the Environment Canada's global trajectory model (GTM), have shown that low-level northerly winds at 850, 950, and 1000 hPa levels (we present only the 850 hPa data in Figures 5a–5d) frequently passed across the Northern High Dust Desert (a major source of Asian dust with Badan Juran Desert as its center). The second major dust source, the Western High Dust Desert with Takelimakan Desert as its center, experienced fewer trajectories passing across it (Figures 5a–5d).

[31] Five general pathways of surface trajectories that passed over Beijing during spring 2001 (denoted by colors in Figure 5d) may be identified. The first pathway, labeled "Northeast Sand Land Path" (black line at right of Figure 5d), accounted for ~22% of the total 43 transport paths. Soil dust aerosol was uplifted from the source regions over the sand land in northeastern China, especially through Onqin Daga sand land, and surface northeasterly winds carried them to Beijing. Pathway 2 ("Northerly Mongolia Path") was mainly associated with air passing through and over Mongolia and the north slopes of Ying Mountain and then to Beijing (blue line in Figure 5d, accounting for ~40% of the total paths). The third type of air trajectory was mainly from the Ala Mountain Pass and its surrounding areas, and through the Northern High Dust Desert, along the

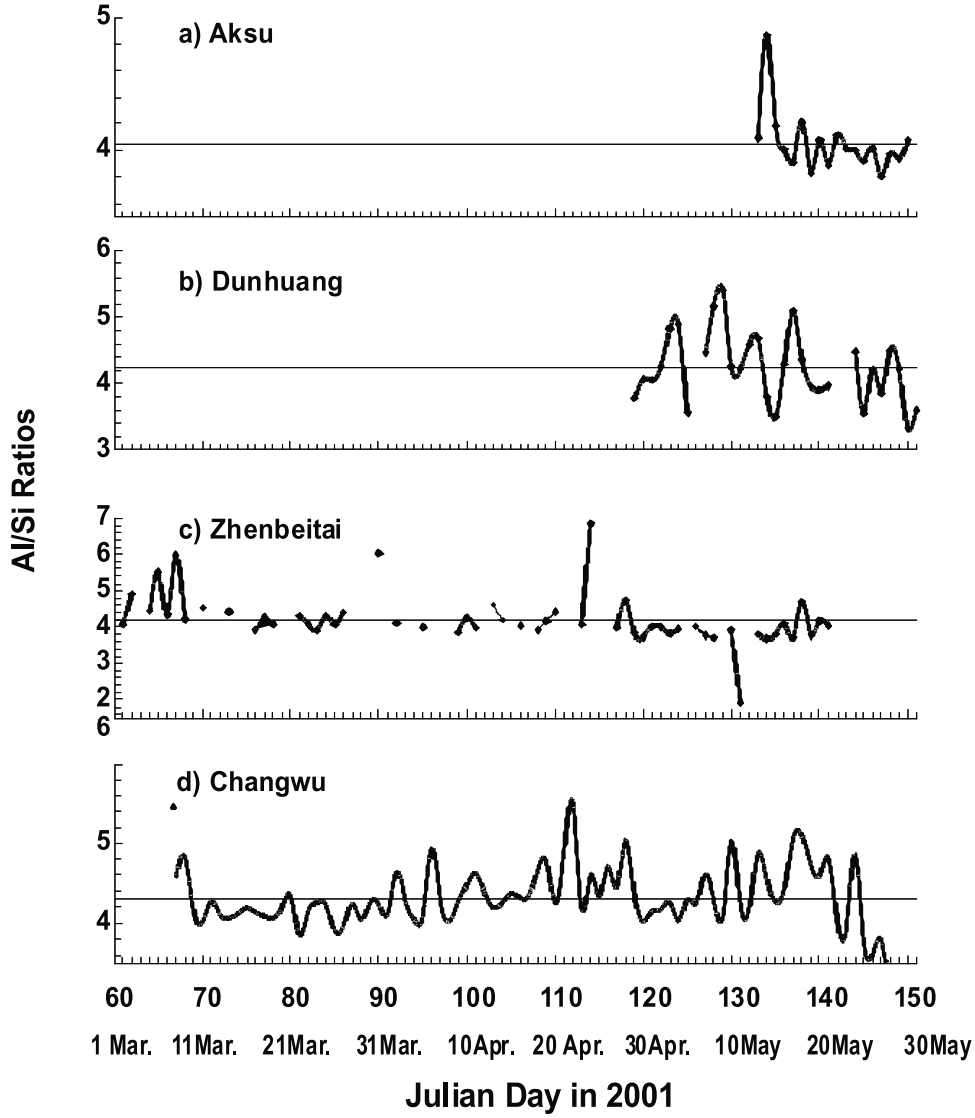

Figure 4. Time series of the Si:Al ratios for (a) Aksu, (b) Dunhuang (c) Zhenbeitai, and (d) Changwu.

south slope of Yin Mountain, passing the areas between Helan Mountain And Yin Mountain and reaching Beijing. This group of air trajectories is called the "Northern Desert Path" (mauve line in Figure 5d) and accounts for ~25% of the total paths. A fourth trajectory occurred only one time in 2001 for dust to Beijing, and originated from the Western High Dust Desert and moved easterly to Beijing (Western Desert Path, the green line in Figure 5d). The final pathway (bold red line in Figure 5d) occurred five times in 2001 and reached Beijing from the south, and then turning directions, often passing through the southern and northern mountain passes of Taihang Mountain and then moving north to Beijing (called "turning path") accounting for ~11% of the total paths.

[32] The transport pathways of soil dust to Changwu (Figure 5a) and XiAn (Figure 5b) are similar to those for Beijing with the same two major pathways: Northern Chinese Desert Path and Western Chinese Desert Path, respectively. However, when these two air masses move out of the mountain passes between Yin Mountain and Helan Mountain, Helan Mountain and Liupan Mountain, and Liuliang Mountain, and move over the Helan Mountain, they branch southward to Changwu and XiAn instead of to Beijing. There also exists another interesting path to XiAn and Changwu (shown with bold red line in Figures 5a and 5b). This passes over the sand land of northeastern China, moves southward along the western part of Taihang Mountain, travels through the mountain pass between Taihang Mountain and Qingling Mountain, and then moves northwestward to XiAn and Changwu.

[33] At ZBT, Yulin (Figure 5c), the Northeast Sand Land Path (back line), Northern Desert Path (mauve line), and Western Desert Path (green line) dominated during spring of 2001.

3.4. Size Distribution of Vertical Dust Flux

[34] In addition to the bulk TSP samples, six and eight size-segregated samples were also collected under DS events at DH and ZBT, respectively, using a Battle type cascade impactor (PIXE International Corporation, Talla-

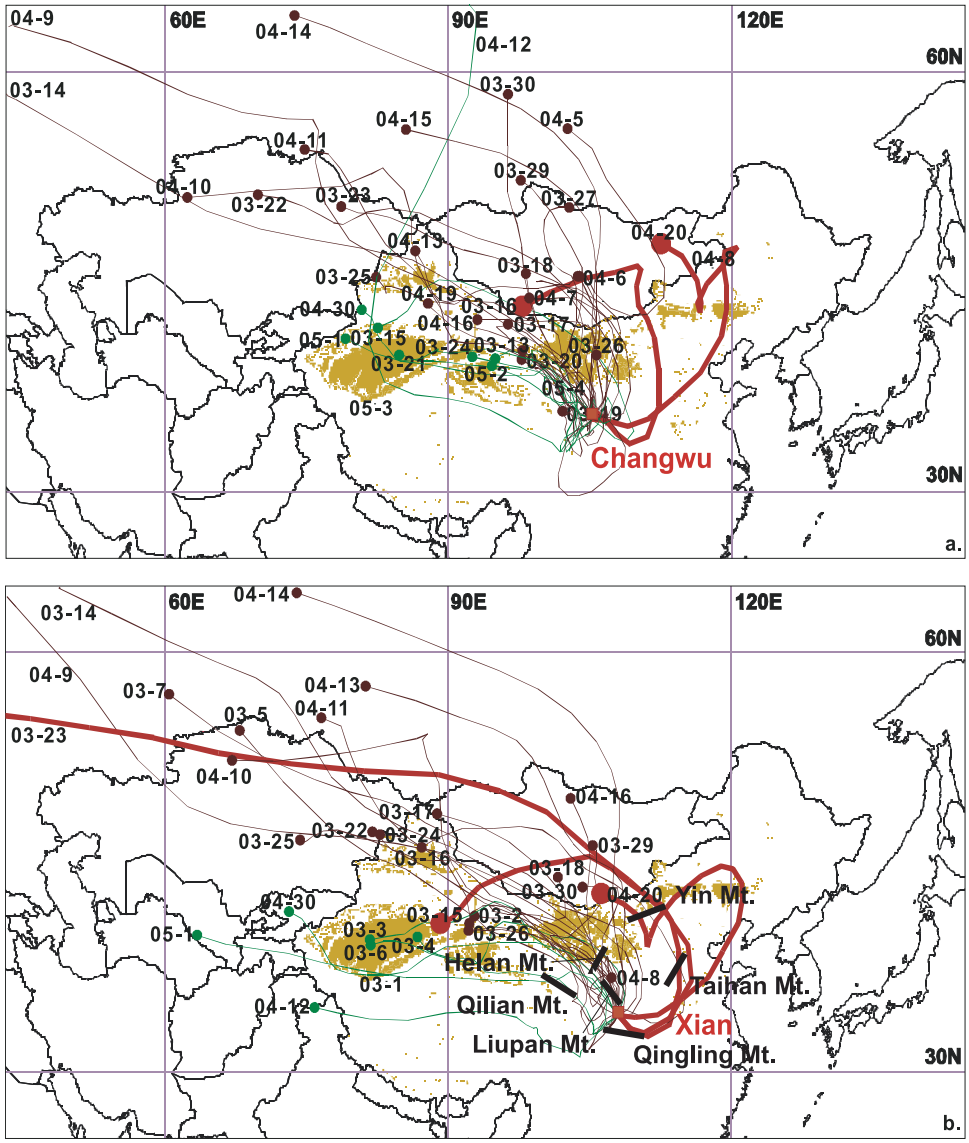

Figure 5. A 120-hour air mass backward-trajectory analyses at 850 mbar, 0600 UTC for (a) Changwu, (b) XiAn, (c) ZBT, and (d) Beijing. Black and blue lines denote the Northeast Sand Land Path and Northerly Mongolia Path for the dust transport, respectively. Northern Desert Path and Western Desert Path are shown by mauve and green lines, respectively. The bold red lines represent Turning Path. Six major mountain ridges are marked approximately as black lines on Figures 5b and 5d for Yin, Taihan, Qingling, Liupan, Helan, and Qilian Mountains.

hassee, Florida). Eight size bins from <0.25, 0.25–0.5, 0.5–1, 1–2, 2–4, 4–8, 8–16, and >16 μm in aerodynamic equivalent diameters (AED) were used to measure the dust particle size distributions. Subsequent chemical analysis yielded the elemental composition for each size range. The sums of the eight size-segregated elemental data, Si, for instance, shown by open triangles in Figures 3b and 3c, are generally consistent with bulk data, demonstrating the internal consistency of the measurements. Mass-size distributions (MSDs) of Si and Al are shown in Figure 6 for the 20 DS samples from the source regions, together with the previous data for six DS samples collected at Aksu, Qira (at the southern margin of Takliamakan Desert, 37°6′N, 82°34′E) and Jartai (a desert site at Ulan Buh Desert, 40°34′N, 106°34′E) in 1994 [*Zhang et al.*, 1997]. This allows the derivation of the size distribution of vertical dust flux. In general, the two typical dust-derived elements (Al and Si) exhibit comparable MSDs, and were comparable among all samples (Figure 6). This suggests similarities in Asian dust particles ejected from source regions.

[35] The MSDs of the two dust elements (Al and Si) from our observations were found to be approximately lognormal in the range 0.25–16 μm over the source regions. A fitting of MSDs for the Si and Al was performed using a least squares linear regression between standard normal deviate (SND) and the natural logarithm of the particle diameter (lnD) previously described by *Dulac et al.* [1989]. According to *Patterson and Gillette* [1977], the particle-size distributions of mineral dust are usually considered to consist of three modes: background, normal, and coarse mode, each

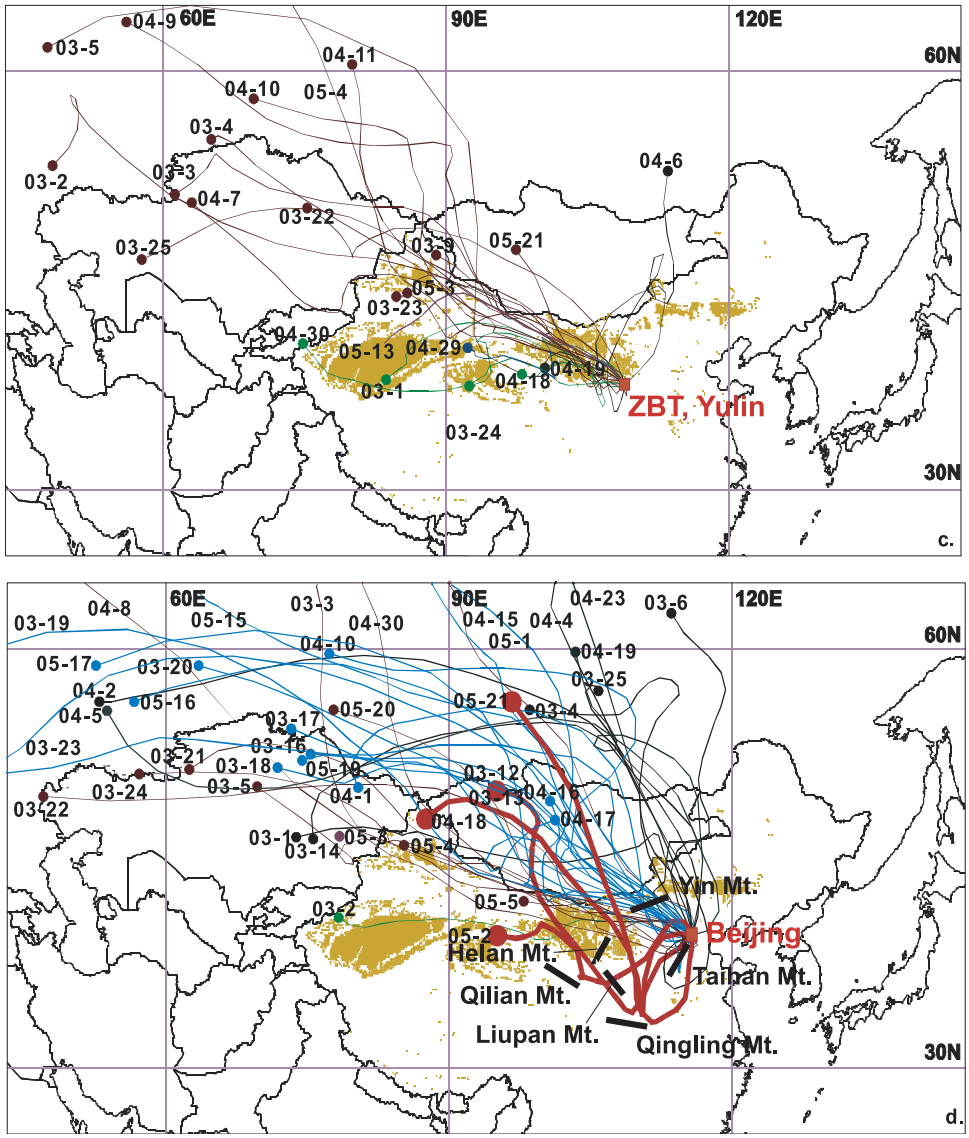

Figure 5. (continued)

characterized by a lognormal size distribution, with size ranges of about 20–200, 2–20, and 0.04–1 μm in diameters. As our impactor has a cutoff size of <0.25 μm in stage 1 for the background mode (<1 μm) and of >16 μm in stage 7 for the coarse mode (>20 μm) , our desert-sample MSD data (Figure 6) provides a way to assess the relative importance of giant and submicrometer dust particles in terms of dust loads.

[36] On the basis of correlation coefficients of the least squares linear regressions, the lognormal fitting of the two elemental MSDs between 0.25 and16 μm to our desert-sample data was satisfactory at the <5% probability level for 40 of 40 element/particle-size distributions. The σ_g of the curves was less than 2 (100% each for Si and Al). These results indicate that there were generally minor impacts of the background mode particles [*Arimoto et al.*, 1985; *Dulac et al.*, 1989; *Zhang et al.*, 1993] on the MSDs for each of these elements observed at the source regions of Asian dust.

[37] The average weight percent for the two elements in each of the three particle-size fractions was observed and calculated from the fitted MSD curves (Table 4). The reconstructed size spectra show that the dominant mass of the soil dust aerosols in these locally occurring DS events was for particles with diameters from 0.25 to 16 μm, which accounted for about 69% of the total mineral aerosol mass (Table 4). The fine and coarse dust modes contribute about 1.7 and 30%, respectively (Table 4). These indicate that a coarse particle fraction exists in the near-surface atmosphere in the DS dust at source regions. This could be important for simulation of dust particle transport especially in the near-source areas.

4. Conclusions

[38] Observations of aerosol chemical and physical properties made at the China Dust Storm Research network of ground stations provide a 3-month data set of Asian dust during the intensive observation period of ACE-Asia. This is the first time that such a comprehensive data set, including aerosol and Asian dust mass, dust and nondust elemen-

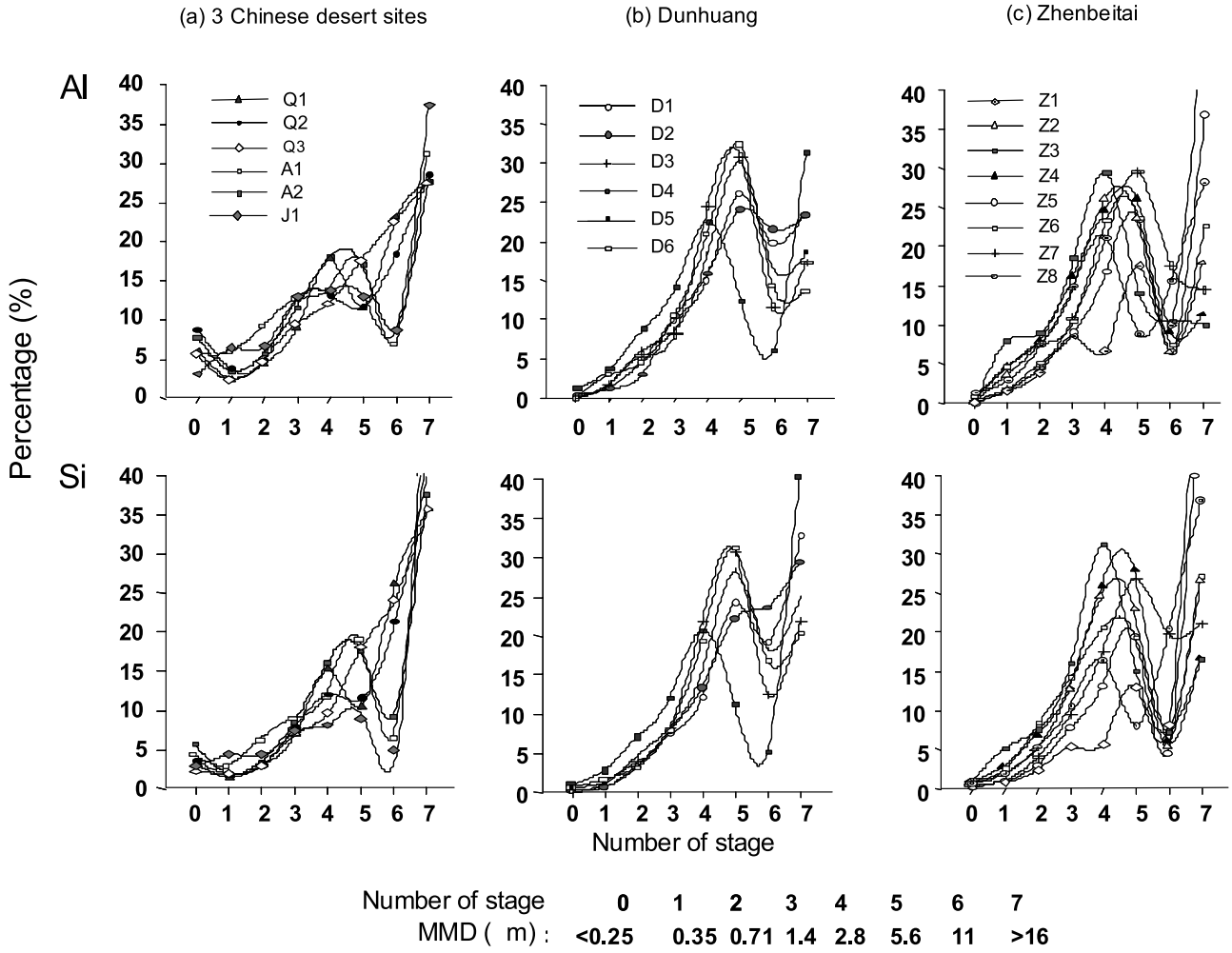

Figure 6. Mass size distributions (MSDs) of two typical dust elements, aluminum (top) and silicon (bottom), in 20 aerosol particles collected at 10–20 m surface atmosphere from five Chinese desert sites during the local dust storm events: (a) for desert sites Arksu, Qira, and Jartai, (b) for Dunhuang, and (c) for Zhenbaitai. The legends in the figures such as A1 and Z8 are sample numbers.

tal concentrations, proportion of all dust elements, transport paths and surface PDSs during DS events, has been reported for hyperarid, semiarid, urban, and rural areas of China. Five major transport pathways of Asian dust storm were identified during this period of time through a back-trajectory analysis.

[39] In general, spring aerosol particles over northern China were composed mainly of Asian dust with a percentage contribution of 45% at Aksu, 67% at DH, 69% at CW, and 82% at ZBT (where only northerly winds were sampled) to the total aerosol mass during DS and N-DS conditions, respectively. The elemental composition (Al, Ca, Cr, Fe, K, Mn, Mg, Si, Ti, V, and Zn) of aerosol particles was dominated by dust particles, even though some elements are typically anthropogenically derived in mainland China. Under both DS and N-DS conditions, the weight percentages of typical dust elements, Al, Ca, Fe, Mg, Mn, K, Si, and Ti, were obtained for the Western High Dust Desert, Northern High Dust Deserts and the Loess Plateau. The percentages of Ca, Fe, and Mg were 12, 6, and 3%, respectively, for Asian dust particles from the Western High Dust Desert. The weight percent of Si for dust aerosol from Northern High Dust Desert is relatively higher than from the Western desert. This indicates that the inhomogeneity of sources for Asian dust had more influence on Ca, Si, Fe, and Mg than on Al, K, Mn, and Ti.

[40] On the basis of the durations for which both TSP and dust elemental loads exceeded spring daily average levels, four major DS episodes were identified. Beijing had relatively higher average PM-10 levels than XiAn, Yinchuan and CW TSP and 43 dust days compared with 32 days in XiAn in spring 2001.

Table 4. Mean Size Distribution of Dust Aerosol During Local Dust-Storm Events (20 Ground-Based Aerosol Samples Collected From Desert Sites, Aksu, Qira (37°6′N, 82°34′E), Jarti (40°34′N, 106°34′E), Dunhuang and Yulin, in Spring of 1994 and 2001)

Size Distribution (d, μm) (Mean of Al and Si Data)				
<0.25	0.25 to 16 (Lognormal Distribution)			>16
%	MMD[a]	σ[b]	%	%
1.7	4.5	1.5	69	30

[a]Mass mean diameter.
[b]Standard deviation of the lognormal distribution.

[41] During the nondust storm (N-DS) days, when calm or weak wind conditions prevailed, the monthly mean background aerosol concentrations were from 130 to 150 $\mu g\ m^{-3}$ in March and April, respectively, and 80 $\mu g\ m^{-3}$ in May, at CW. Thereafter, these background TSP loadings were about 60, 40, and 50 $\mu g\ m^{-3}$ during June, July, and August of 2001. At the desert source site (ZBT), in comparison with the DS data, nondusty days with calm or weak northwesterly or northeasterly winds had background aerosol loadings of 93 $\mu g\ m^{-3}$ in March, 150 $\mu g\ m^{-3}$ in April, and 91 $\mu g\ m^{-3}$ in May.

[42] Aluminium and silicon concentration data from cascade impactor samples at five desert sites in China have been used to derive the mass-particle size distributions. These are probably the best available data for aerosol size distributions close to the dust source regions. These results show evidence for two modes in the dust particle size distribution, with one maximum occurring in stages 3–5 (1–8 μm AED) and a second maximum in stage 7 (>16 μm AED). These data suggest that the dust sampled at each of these sites is a combination of dust transported from long distances, which is concentrated in the smaller peak, and locally generated material, which forms the larger peak.

[43] The complete time series of TSP in spring 2001 and physical/chemical properties of soil dust in source regions provide a valuable data set to be used for soil dust model inputs and validations. Application of this data set is presented in our companion simulation paper [*Gong et al.*, 2003].

[44] **Acknowledgments.** This research was supported by grants from the Chinese Academy of Sciences (CAS) (KZCX2-305), National Key Project of Basic Research (G2000048703), NSF of China (40121303 and 49825105) and a special Ph.D. fund from the CAS. We thank Ian McKendry of the University of British Columbia, Canada, for providing valuable comments on the manuscript.

References

Andreae, M. O., Climate effects of changing atmospheric aerosol levels, in *World Survey of Climatology: Future Climates of the World*, edited by A. Henderson-Sellers, pp. 341–392, Elsevier Sci., New York, 1995.

Arimoto, R., R. A. Duce, B. J. Ray, and C. K. Unni, Atmospheric trace elements at Enewetak Atoll: 2. Transport to the ocean by wet and dry deposition, *J. Geophys. Res.*, *90*, 2391–2408, 1985.

Dulac, F., P. Buat-Ménard, S. M. U. Ezat, and G. Bergametti, Atmospheric input of trace metals to the western Mediterranean: Uncertainties in modelling dry deposition from cascade impactor data, *Tellus, Ser. B*, *41*, 362–378, 1989.

Gong, S. L., X. Y. Zhang, T. L. Zhao, I. G. McKendry, D. A. Jaffe, and N. M. Lu, Characterization of soil dust aerosol in China and its transport and distribution during 2001 ACE-Asia: 2. Model simulation and validation, *J. Geophys. Res.*, *108*, doi:10.1029/2002JD002633, in press, 2003.

Geological Soil Standard, Preparation of geochemical standard reference samples (GSR1-6, GSS1-8, GSD9-12), Natl. Bur. of Chem. Explor. Anal., Beijing, China, 1984.

Intergovernmental Panel on Climate Change (IPCC), C*limate Change 2001: The Scientific Basis-Contribution of Working Group I to the Third Assessment Report of the Intergovernmental Panel on Climate Change*, Cambridge Univ. Press, New York, 2001.

Merrill, J. T., M. Uematsu, and R. Bleck, Meteorological analysis of long-range transport of mineral aerosol over the North Pacific, *J. Geophys. Res.*, *94*, 8584–8598, 1989.

Merrill, J. T., E. Arnold, M. Leinen, and C. Weaver, Mineralogy of aeolian dust reaching the North Pacific Ocean: 2. Relationship of mineral assemblages to atmospheric transport patterns, *J. Geophys. Res.*, *99*, 21,025–21,032, 1994.

Overpeck, J., D. Rind, A. Lacis, and R. Healy, Possible role of dust-induced regional warming in abrupt climate change during the last glacial period, *Nature*, *384*, 447–449, 1996.

Patterson, C. C., and D. A. Gillette, Commonalities in measured size distributions for aerosols having a soil-derived component, *J. Geophys. Res.*, *82*, 2074–2082, 1977.

Prospero, J. M., Eolian transport to the world ocean, in *The Sea*, edited by C. Emiliani, pp. 801–874, John Wiley, New York, 1981.

Sokolik, I. N., D. M. Winker, G. Bergametti, D. A. Gillette, G. Carmichael, Y. J. Kaufman, L. Gomes, L. Schuetz, and J. E. Penner, Introduction to special section on mineral dust: Outstanding problems in quantifying the radiative impacts of mineral dust, *J. Geophys. Res.*, *106*, 18,015–18,027, 2001.

Solomon, P. A., T. Fall, L. Salmon, G. R. Cass, H. A. Gray, and A. Davision, Chemical characteristics of PM10 aerosols collected in the Los Angeles Area, *J. Air Pollut. Control Assoc.*, *39*, 154–163, 1989.

Taylor, S. R., and S. M. McLennan, The geochemical evolution of the continental crust, *Rev. Geophys.*, *33*, 241–265, 1995.

Tegen, I., A. L. Andrew, and I. Fung, The influence on climate forcing of mineral aerosols from disturbed soils, *Nature*, *380*, 419–422, 1996.

Zhang, D. E., Synoptic-climatic studies of dust fall in China since the historic times, *Sci. Sin.*, *27*(8), 825–836, 1984.

Zhang, X., R. Arimoto, Z. An, T. Chen, G. Zhu, and X. Wang, Atmospheric trace elements over source regions for Chinese dust: Concentrations, sources and atmospheric deposition on the Loess Plateau, *Atmos. Environ., Part A*, *27*, 2051–2067, 1993.

Zhang, X. Y., G. Y. Zhang, G. H. Zhu, D. E. Zhang, Z. S. An, T. Chen, and X. P. Huang, Elemental tracers for Chinese source dust, *Sci. China, Ser. D*, *39*(5), 512–521, 1996.

Zhang, X. Y., R. Arimoto, and Z. S. An, Dust emission from Chinese desert sources linked to variations in atmospheric circulation, *J. Geophys. Res.*, *102*, 28,041–28,047, 1997.

Zhang, X. Y., R. Arimoto, G. H. Zhu, T. Chen, and G. Y. Zhang, Concentration, size-distribution and deposition of mineral aerosol over Chinese desert regions, *Tellus, Ser. B*, *50*, 4317–4331, 1998.

Zhang, X. Y., R. Arimoto, and Z. S. An, Glacial and interglacial patterns for Asian dust transport, *Quat. Sci. Rev.*, *18*, 811–819, 1999.

Zhang, X. Y., J. J. Cao, L. M. Li, R. Arimoto, Y. Cheng, B. Huebert, and D. Wang, Characterization of atmospheric aerosol over XiAn in the south margin of the Loess Plateau, China, *Atmos. Environ.*, *36*, 4189–4199, 2002.

Y. Cheng, F. M. Mei, Z. X. Shen, D. Wang, Y. Q. Wang, and X. Y. Zhang, State Key Laboratory of Loess and Quaternary Geology, Institute of Earth Environment, Chinese Academy of Sciences, 10 Fenghui S. Road, P.O. Box 17, XiAn 710075, China.

S. L. Gong, Air Quality Research Branch, Meteorological Service of Canada, 4905 Dufferin Street, Toronto, Ontario, Canada M3H 5T4. (sunling.gong@ec.gc.ca)

L. C. Liu, Institute of Cold and Arid Environment and Engineering Research, Chinese Academy of Sciences, Donggang W. Road, Lanzhou 730000, China.

X. X. Xi, College of Resource and Environment, Lanzhou University, 298 Tianshui Road, Lanzhou 730000, China.

Z. J. Zhou, Climate Data Centre, National Meteorological Canter, China Metrology Administration, 46 Baishiqiao Road, Beijing 100081, China.